

# Sidelobe Suppression for Capon Beamforming with Mainlobe to Sidelobe Power Ratio Maximization

Yipeng Liu, and Qun Wan

## Abstract

High sidelobe level is a major disadvantage of the Capon beamforming. To suppress the sidelobe, this paper introduces a mainlobe to sidelobe power ratio constraint to the Capon beamforming. It minimizes the sidelobe power while keeping the mainlobe power constant. Simulations show that the obtained beamformer outperforms the Capon beamformer.

## Index Terms

array signal processing, Capon beamforming; sidelobe suppression

## I. INTRODUCTION

**A** beamformer is a multiple antennas system which makes spatial beam focused on the target direction and spatial beam nulled interference signal. In this system, each transmit antenna is weighted by a properly designed gain and phase shift before transmission. It is used extensively to improve the performance in a variety of areas such as radar, sonar and wireless communications [1].

The Capon beamformer is one of the most popular beamforming systems. It is a data-dependent beamformer which minimizes the array output power subject to the linear constraint that the signal-

Yipeng Liu and Qun Wan are with the Electronic Engineering Department, University of Electronic Science and Technology of China, Chengdu, 611731, China. Yipeng Liu is also a visiting researcher with Electronic Engineering Department of the Electronic Engineering Department, Tsinghua University, 100084, China. e-mail: (liuyipeng@uestc.edu.cn; wanqun@uestc.edu.cn);.

Manuscript received Month Day, 2011; revised Month Day, Year.

of-interest (SOI) does not suffer from any distortion by adaptive selection of the weight vector. The Capon beamformer has better resolution and much better interference rejection capability than the data-independent beamformer. However, its high sidelobe level and the SOI steering vector uncertainty due to differences between the assumed signal arrival angle and the true arrival angle would seriously degenerate the performance in the presence of environment noise and interferences [1], [2], [3].

With a spherical uncertainty set was introduced, doubly constrained robust (DCR) Capon beamformer is obtained with the increased robustness against DOA mismatch [4]. To achieve a faster convergence speed and a higher steady state signal to interference plus noise ratio (SINR), [5] constrains its weight vector to a specific conjugate symmetric form. In [6], by iteratively estimation of the actual steering vector based on conventional RCB formulation, iterative robust capon beamformer (IRCB) with adaptive uncertainty level is proposed to enhance the robustness against DOA mismatch.

Many works have been done to enhance the robustness against the SOI steering vector uncertainty, to accelerate the convergence, etc [7]. However, no constraint is put onto the interference and background noise. Based on the Capon criterion, a new constraint is added to maximize the mainlobe and sidelobe power ratio (MSPR) to shape the beam pattern. As more power is accumulated in the mainlobe area, the robustness against SOI steering vector uncertainty is improved; and as less power is in the sidelobe area, the interference and noise rejection capability can be enhanced. Therefore, a better performance can be achieved. Numerical Results also demonstrate that the proposed beamformer outperforms.

## II. SIGNAL MODEL

The signal impinging into a uniform linear array (ULA) with  $M$  antennas can be represented by an  $M$ -by-1 vector [1]:

$$\mathbf{x}(k) = s(k)\mathbf{a}(\theta_0) + \sum_{j=1}^J \beta_j(k)\mathbf{a}(\theta_j) + \mathbf{n}(k) \quad (1)$$

where  $k$  is the index of time,  $J$  is the number of interference sources,  $s(k)$  and  $\beta_j(k)$  (for  $j = 1, \dots, J$ ) are the amplitudes of the signal of interest (SOI) and interfering signals at time instant  $k$ , respectively,  $\theta_l$

(for  $l = 0, 1, \dots, J$ ) are the direction of arrivals (DOAs) of the SOI and interfering signals,  $\mathbf{a}(\theta_l) = \begin{bmatrix} 1 & \exp(j\varphi_l) & \cdots & \exp(j(M-1)\varphi_l) \end{bmatrix}^T$  (for  $l = 0, 1, \dots, J$ ) are the steering vectors of the SOI and interfering signals, wherein  $\varphi_l = (2\pi d/\lambda) \sin \theta_l$ , with  $d$  being the distance between two adjacent sensors and  $\lambda$  being the wavelength of the SOI; and  $\mathbf{n}(k)$  is the additive white Gaussian noise (AWGN) vector at time instant  $k$ .

The output of a beamformer for the time instant  $k$  is then given by:

$$y(k) = \mathbf{w}^H \mathbf{x}(k) = s(k) \mathbf{w}^H \mathbf{a}(\theta_0) + \sum_{j=1}^J \beta_j(k) \mathbf{w}^H \mathbf{a}(\theta_j) + \mathbf{w}^H \mathbf{n}(k) \quad (2)$$

where  $\mathbf{w}$  is the  $M$ -by-1 complex-valued weighting vector of the beamformer.

### III. THE PROPOSED BEAMFORMER

The Capon beamformer is defined as the solution to the following linearly constrained minimization problem [1]:

$$\mathbf{w}_{Capon} = \arg \min_{\mathbf{w}} \left( \mathbf{w}^H \mathbf{R}_x \mathbf{w} \right), \text{ s.t. } \mathbf{w}^H \mathbf{a}(\theta_0) = 1 \quad (3)$$

where  $\mathbf{R}_x$  is the  $M$ -by- $M$  covariance matrix of the received signal vector  $\mathbf{x}(k)$ , and  $\mathbf{w}^H \mathbf{a}(\theta_0) = 1$  is the distortionless constraint applied on the SOI.

In the perspective of the beam pattern, it is observed from the Capon beamformer (3) that there is only an explicit constraint on the desired DOA, i.e.  $\mathbf{w}^H \mathbf{a}(\theta_0) = 1$ , while no constraint is put onto the interference and background noise. To repair this drawback, we propose the following cost function with a regularization term, which forces maximization of the MSPR:

$$\mathbf{w}_{MSPR} = \arg \min_{\mathbf{w}} \left\{ \mathbf{w}^H \mathbf{R}_x \mathbf{w} + \gamma \left[ \left( \|\mathbf{w}^H \mathbf{A}_M\|_2^2 - 1 \right)^2 + \|\mathbf{w}^H \mathbf{A}_S\|_2^2 \right] \right\} \quad (4)$$

s.t.  $\mathbf{w}^H \mathbf{a}(\theta_0) = 1$

where  $\gamma$  is the weighting factor balancing the minimum variance constraint and the MSPR minimization constraint. The  $M$ -by- $N$   $\mathbf{A}$  is the array manifold with  $\alpha_n$  ( $n = 1, 2, \dots, N$ ) being the sampled angles in the  $[-90^\circ, 90^\circ]$ , and the  $N$  steering vectors cover all the DOAs in the sampling range, with  $\alpha_0$  being

the DOA of the SOI as defined in (1), i.e.,

$$A_{mn} = \exp(j(m-1)\varphi_n), \text{ for } m = 1, \dots, M; n = 1, \dots, N \quad (5)$$

$$\varphi_n = \frac{2\pi d}{\lambda} \sin \alpha_n, \text{ for } n = 1, \dots, N \quad (6)$$

$$\mathbf{A}_M = \begin{bmatrix} \mathbf{a}(\theta_{-b}) & \cdots & \mathbf{a}(\theta_0) & \cdots & \mathbf{a}(\theta_{+b}) \end{bmatrix} \quad (7)$$

$$\mathbf{A}_S = \begin{bmatrix} \mathbf{a}(\theta_{-90}) & \cdots & \mathbf{a}(\theta_{-b-1}) & \mathbf{a}(\theta_{+b+1}) & \cdots & \mathbf{a}(\theta_{+90}) \end{bmatrix} \quad (8)$$

$\mathbf{A}_S$  is sub-matrix of the steering matrix  $\mathbf{A}$ , and it is constituted with the sidelobe steering vectors in  $\mathbf{A}$ .  $\mathbf{A}_M$  is sub-matrix of the steering matrix  $\mathbf{A}$  too, and it is constituted with the mainlobe steering vectors in  $\mathbf{A}$ .  $b$  is an integer corresponding to the bounds between the mainlobe and the sidelobe of the beam pattern.

The product  $\mathbf{w}^H \mathbf{A}_S$  indicates array gains of the sidelobe; and the product  $\mathbf{w}^H \mathbf{A}_M$  indicates array gains of the mainlobe. The newly added MSPR  $\left( \|\mathbf{w}^H \mathbf{A}_M\|_2^2 - 1 \right)^2 + \|\mathbf{w}^H \mathbf{A}_S\|_2^2$  is minimized to minimize the sidelobe power  $\|\mathbf{w}^H \mathbf{A}_S\|_2^2$  while enforcing the mainlobe power to be a constant. Thus, the MSPR  $\|\mathbf{w}^H \mathbf{A}_M\|_2^2 / \|\mathbf{w}^H \mathbf{A}_S\|_2^2$  would be maximized.

The proposed optimization model can be solved efficiently by Lagrange multiplier method. First the Lagrange multipliers technique is used to combine the constraints in (4) into the objective function:

$$\begin{aligned} f(\mathbf{w}) &= \mathbf{w}^H \mathbf{R}_x \mathbf{w} + \gamma \left( \|\mathbf{w}^H \mathbf{A}_M\|_2^2 - 1 \right)^2 \\ &\quad + \gamma \|\mathbf{w}^H \mathbf{A}_S\|_2^2 + \mu \left( \mathbf{w}^H \mathbf{a}(\theta_0) - 1 \right) \\ &= \mathbf{w}^H \mathbf{R}_x \mathbf{w} + \gamma \left( \mathbf{w}^H \mathbf{A}_M \mathbf{A}_M^H \mathbf{w} - 1 \right)^2 \\ &\quad + \gamma \mathbf{w}^H \mathbf{A}_S \mathbf{A}_S^H \mathbf{w} + \mu \left( \mathbf{w}^H \mathbf{a}(\theta_0) - 1 \right) \end{aligned} \quad (9)$$

Thus, we have:

$$\begin{aligned} \frac{\partial f(\mathbf{w}, \mu)}{\partial \mathbf{w}^H} &= \mathbf{R}_x \mathbf{w} + \gamma \left( \mathbf{w}^H \mathbf{A}_M \mathbf{A}_M^H \mathbf{w} - 1 \right) \left( 2 \mathbf{A}_M \mathbf{A}_M^H \mathbf{w} \right) \\ &+ \gamma \mathbf{A}_S \mathbf{A}_S^H \mathbf{w} + \mu \mathbf{a}(\theta_0) \end{aligned} \quad (10)$$

$$\frac{\partial f(\mathbf{w}, \mu)}{\partial \mu} = \mathbf{w}^H \mathbf{a}(\theta_0) = 1 \quad (11)$$

From (10),

$$\left( \mathbf{R}_x + \gamma \left( 2 \mathbf{w}^H \mathbf{A}_M \mathbf{A}_M^H \mathbf{w} - 2 \right) \mathbf{A}_M \mathbf{A}_M^H + \gamma \mathbf{A}_S \mathbf{A}_S^H \right) \mathbf{w} = -\mu \mathbf{a}(\theta_0) \quad (12)$$

$$\mathbf{w} = -\mu \left( \mathbf{R}_x + \gamma \left( 2 \mathbf{w}^H \mathbf{A}_M \mathbf{A}_M^H \mathbf{w} - 2 \right) \mathbf{A}_M \mathbf{A}_M^H + \gamma \mathbf{A}_S \mathbf{A}_S^H \right)^{-1} \mathbf{a}(\theta_0) \quad (13)$$

Substituting (13) into (11) gives:

$$-\mu \mathbf{a}(\theta_0)^H \Xi \mathbf{a}(\theta_0) = 1 \quad (14)$$

where

$$\Xi = \left( \left( \mathbf{R}_x + \gamma \left( 2 \mathbf{w}^H \mathbf{A}_M \mathbf{A}_M^H \mathbf{w} - 2 \right) \mathbf{A}_M \mathbf{A}_M^H + \gamma \mathbf{A}_S \mathbf{A}_S^H \right)^H \right)^{-1} \quad (15)$$

Then,

$$\mu = \frac{-1}{\mathbf{a}(\theta_0)^H \Xi \mathbf{a}(\theta_0)} \quad (16)$$

Substituting (16) into (13), gives:

$$\mathbf{w} = \frac{\Xi \mathbf{a}(\theta_0)}{\mathbf{a}(\theta_0)^H \Xi \mathbf{a}(\theta_0)} \quad (17)$$

Therefore, the iterative algorithm is:

$$\begin{aligned} &\mathbf{w}(i+1) \\ &= \frac{\left( \mathbf{R}_x + \gamma \left( 2 \mathbf{w}(i)^H \mathbf{A}_M \mathbf{A}_M^H \mathbf{w}(i) - 2 \right) \mathbf{A}_M \mathbf{A}_M^H + \gamma \mathbf{A}_S \mathbf{A}_S^H \right)^{-1} \mathbf{a}(\theta_0)}{\mathbf{a}(\theta_0)^H \left( \left( \mathbf{R}_x + \gamma \left( 2 \mathbf{w}(i)^H \mathbf{A}_M \mathbf{A}_M^H \mathbf{w}(i) - 2 \right) \mathbf{A}_M \mathbf{A}_M^H + \gamma \mathbf{A}_S \mathbf{A}_S^H \right)^H \right)^{-1} \mathbf{a}(\theta_0)} \end{aligned} \quad (18)$$

where  $i$  denotes the interaction index.

#### IV. SIMULATION

In the simulations, a ULA with 8 half-wavelength spaced antennas is considered. The AWGN at each sensor is assumed spatially uncorrelated. The DOA of the SOI is set to be  $0^\circ$ , and the DOAs of three interfering signals are set to be  $-30^\circ$ ,  $30^\circ$ , and  $70^\circ$ , respectively. The signal to noise ratio (SNR) is set to be 10 dB, and the interference to noise ratios (INRs) are assumed to be 20 dB, 20 dB, and 40 dB in  $-30^\circ$ ,  $30^\circ$ , and  $70^\circ$ , respectively. 100 snapshots are used for each simulation. Without loss of generality,  $b$  is set to be 12,  $\gamma$  is chosen to be 1. The matrix  $\mathbf{A}$  consists of all steering vectors in the DOA range of  $[-90^\circ, 90^\circ]$  with the sampling interval of  $1^\circ$ .

To examine its influence on the performance, the SINR is calculated via the following formula:

$$SINR = \frac{\sigma_s^2 \mathbf{w}^H \mathbf{a}(\theta_0) \mathbf{a}^H(\theta_0) \mathbf{w}}{\mathbf{w}^H \left( \sum_{j=1}^J \sigma_j^2 \mathbf{a}(\theta_j) \mathbf{a}^H(\theta_j) + \mathbf{Q} \right) \mathbf{w}} \quad (19)$$

where  $\sigma_s^2$  and  $\sigma_j^2$  are the variances of the SOI and  $j$ -th interference,  $\mathbf{Q}$  is a diagonal matrix with the diagonal elements being the noise's variances.

Fig. 1 shows beam patterns of the Capon beamformer (3), the MSPR-Capon beamformer (4) of 1000 Monte Carlo simulations. It is obvious that a better sidelobe suppression performance is achieved by the MSPR-Capon beamformer. The beam pattern of the MSPR-Capon beamformer has a lower array gain level in sidelobe area, and provides deeper nulls in the directions of interference, i.e.,  $-30^\circ$ ,  $30^\circ$ , and  $70^\circ$ , respectively. The average received SINR by the Capon beamformer, the MSPR-Capon beamformer (4) are 3.6809 dB, and 6.5224 dB. Besides when we change the parameter  $\gamma$ , in 1000 Monte Carlo simulations, the influence of choice of the parameter on the output SINR is slight, and all the values of SINR lies between 6.4287dB and 6.7861dB.

Fig. 2 shows beam patterns of the beamformers that we have discussed, with each beamformer having a  $4^\circ$  mismatch between the steering angle and the DOA of the SOI. We can see that the Capon beamformer has a deep notch in  $4^\circ$ , which is the DOA of the SOI. It can be explained by using the fact that the Capon beamformer is designed to minimize the total array output energy subject to a distortionless constraint in

the DOA of the SOI, so when the steering angle is in  $4^\circ$ , instead of  $0^\circ$ , the Capon beam pattern maintains distortionless in  $0^\circ$  while resulting in a deep null in  $4^\circ$ . This observation shows the high sensitivity of the Capon beamformer to steering angle mismatch. Comparing beam patterns of beamformers defined in (3) and (4), we can see that the MSPR-Capon (4) has a high array gain in the DOA of the SOI. Besides, it suppresses sidelobe levels and deepens the nulls for interference avoidance. In the case of  $4^\circ$  mismatch, the average received SINR by the Capon beamformer (3) and the MSPR-Capon (4) are 0.0009 dB and 3.8402 dB respectively. 1000 Monte Carlo simulations show that the influence of choice of the parameter on the output SINR is slight too, and all the values of SINR lie between 3.6571dB and 3.9380 dB.

## V. CONCLUSION

The proposed beamformer introduces a new beam pattern shaping constraint. it shows superiority to the MVDR beamformer. The problems of the Capon beamformer's high sidelobe level as well as sensitivity to SOI steering vector errors are much alleviated. In the future work, the MSPR can be incorporated to other Capon based beamformer, such as DCR Capon beamformer, to further enhance the performance.

## ACKNOWLEDGMENT

This work was supported in part by the National Natural Science Foundation of China under grant 60772146, the National High Technology Research and Development Program of China (863 Program) under grant 2008AA12Z306 and in part by Science Foundation of Ministry of Education of China under grant 109139.

## REFERENCES

- [1] J. Li, and P. Stoica, "Robust adaptive beamforming," New York, NY: Wiley, 2006.
- [2] M. Wax, and Y. Anu, "Performance analysis of the minimum variance beamformer," IEEE Transactions on Signal Processing, Vol.44, No. 4, pp. 928-937, Apr. 1996.
- [3] H. Cox, "Resolving power and sensitivity to mismatch of optimum array processors," Journal of the Acoustic Society of America, Vol. 54, No. 3, pp. 771-785, 1973

- [4] J. Li, P. Stoica, and Z. Wang, "Doubly constrained robust capon beamformer," IEEE Transactions on Signal Processing, Vol.52, No. 9, pp. 2407-2423, Sept. 2004.
- [5] L. Zhang, W. Liu, and R. J. Langley, "A minimum variance beamformer with linear and quadratic constraints based on uniform linear antenna arrays," Antennas and Propagation Conference 2009 (LAPC 2009), Loughborough, 16-17 Nov. 2009, pp. 585-588.
- [6] J. P. Lie, X. H. Li, W. Ser, C. S. See, and L. Lei, "Adaptive uncertainty based iterative robust capon beamformer," 2010 IEEE International Conference on Acoustics Speech and Signal Processing (ICASSP2010), March 14 - 19, 2010 - Dallas, Texas, USA, pp. 2526-2529.
- [7] L. Du, T. Yardibi, J. Li, and P. Stoica, "Review of user parameter-free robust adaptive beamforming algorithms," Digital Signal Processing, Vol.19, No. 4, pp. 567-582, 2009.
- [8] G. H. Golub, and C. F. Van Loan, Matrix computation, Baltimore, Maryland, USA: The Johns Hopkins University Press, 1996.

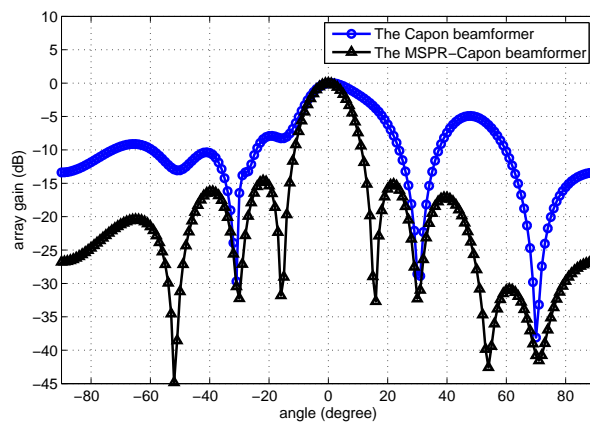


Fig. 1. Normalized beam patterns of the Capon beamformer, and the MSPR-Capon beamformer, without mismatch between the steering angle and the DOA of the SOI.

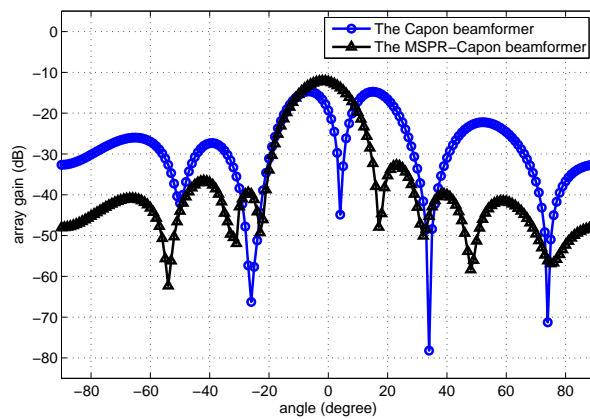


Fig. 2. Normalized beam patterns of the Capon beamformer and the MSPR-Capon beamformer, with 4° mismatch between the steering angle and the DOA of the SOI.